Cis-regulatory code for determining the action of Foxd as both an activator and a repressor in ascidian embryos

Shinichi Tokuhiro and Yutaka Satou

Department of Zoology, Graduate School of Science, Kyoto University,

Kyoto 606-8502, Japan.

Correspondence to Yutaka Satou (yutaka@ascidian.zool.kyoto-u.ac.jp)

Abstract

In early embryos of *Ciona*, an invertebrate chordate, the animal-vegetal axis is established by the combinatorial actions of maternal factors. One target of these maternal factors, *Foxd*, is specifically expressed in the vegetal hemisphere and stabilizes the animal-vegetal axis by activating vegetal hemisphere-specific genes and repressing animal hemisphere-specific genes. This dual functionality is essential for the embryogenesis of early ascidian embryos; however, the mechanism by which Foxd can act as both a repressor and an activator is unknown. Here, we identify a Foxd binding site upstream of *Lhx3/4*, which is activated by Foxd, and compare it with a repressive Foxd binding site upstream of *Dmrt.a*. We found that activating sites bind Foxd with low affinity while repressive sites bind Foxd with high affinity. Reporter assays confirm that this qualitative difference between activating and repressive Foxd binding sites is sufficient to change Foxd functionality. We therefore conclude that the outcome of Foxd transcriptional regulation is encoded in cis-regulatory elements.

Keywords: *Ciona*, Foxd, transcription factor

Introduction

Certain transcription factors can function as both activators and repressors, and these factors can be largely categorized into two groups based on how their activities are determined. The activity of the first group is determined by the cellular environment; these factors act as either an activator or a repressor within a given cell. Their functionality can be switched in various ways, including by direct post-translational modification and through interactions with co-factors. For example, Tcf7 acts as an activator when it forms a complex with β-catenin, while it otherwise acts as a repressor (Behrens et al., 1996; Cavallo et al., 1998; Molenaar et al., 1996; Roose et al., 1998). In contrast, transcription factors in the second group can act as activators and repressors within the same cell. For example, glucocorticoid receptor transcription factor binds to two distinct cis-regulatory elements that are called GREs and nGREs; binding to GREs or nGREs results in gene activation or repression, respectively (Meijsing et al., 2009; Surjit et al., 2011). Similarly, FoxD4L1, a Foxd family protein, downregulates genes promoting neural differentiation and upregulates genes maintaining proliferative neural precursors in the neural precursor cells of amphibian embryos (Klein et al., 2013; Neilson et al., 2012). The N-terminal acidic blob region of FoxD4L1 is required for activating targets, and the C-terminal Engrailed homology region-1 domain is required for repressing targets; however, how the function of FoxD4L1 is changed from activation to repression remains unknown.

In ascidians, Foxd similarly performs dual functions in the vegetal hemisphere of early embryos. Specifically, Foxd activates vegetal hemisphere-specific genes and represses animal hemisphere-specific genes. This action stabilizes the animal-vegetal axis, which is initially established by maternal factors (Tokuhiro et al., 2017). In ascidian embryos, zygotic transcription begins between the 8- and 16-cell stages (Oda-Ishii et al., 2018), and different sets

of genes are expressed in the animal and vegetal hemispheres of 16-cell embryos (Oda-Ishii et al., 2016; Rothbächer et al., 2007). At the 16-cell stage, a complex of maternal β-catenin and Tcf7 activates targets including Foxd in the vegetal hemisphere, while maternal Gata.a activates targets in the animal hemisphere. At the 32-cell stage, Foxd participates in the activation of downstream genes including *Lhx3/4* and *Zic-r.b* in the vegetal hemisphere and represses animal hemisphere-specific genes, including *Dmrt.a* and *Dlx.b* (Tokuhiro et al., 2017). Dual functionality of Foxd is thus important for early embryogenesis in ascidians. Here, we reveal that differences in the nucleotide sequences of Foxd binding sites are a key determinant of Foxd action.

Results

Identification of an upstream regulatory region of *Lhx3/4*

To understand what determines whether Foxd will act as an activator, we first analyzed the upstream regulatory region of *Lhx3/4*, which is positively regulated by Foxd (Hudson et al., 2016). We made a series of deletion constructs that contained 1000, 400, 300, 200, and 150 bp-long regions from sequence upstream of the *Lhx3/4* transcription start site. While *Lhx3/4* is expressed in six vegetal cells at the 32-cell stage, the reporter construct containing the 1000 bp-long region was expressed in only 3.65 cells on average; this is because of mosaic incorporation of the reporter construct (Fig. 1A). While expression of the reporter constructs containing the 400, 300, and 200 bp-long regions was comparable with that of the 1000 bp-containing construct, expression of the shortest construct—containing the 150 bp-long region—was significantly reduced. These experiments indicate that there is a critical *cis*-regulatory element located between −200 and −150 relative to the *Lhx3/4* transcription start site.

Next, we searched for putative Foxd binding sites within the 200 bp region upstream of *Lhx3/4* using the Patser program with the position weight matrices (PWMs) for *Ciona* Foxd and human FOXD2. Two sites around −150 and −100 were identified by both PWMs (Fig. 1B). Because the former site overlapped the region between −150 and −200 that had been identified as important for *Lhx3/4* expression in our reporter construct experiments, we first introduced a mutation at this site. We found that this mutation significantly reduced reporter expression (from 3.75 to 2.89 cells on average; Fig. 1A). However, the reduction rate in this mutant construct was smaller than that in the construct containing the 150 bp-long region, which indicated additional elements between −150 and −200. As two additional sites were identified by the *Ciona* PWM alone, we next introduced mutations into all four of the putative Foxd binding sites, which were

present between −52 and −158. We found that these additional mutations further reduced expression (from 3.75 to 1.1 cells on average; Fig. 1A).

The Foxd binding site in the upstream region of *Lhx3/4* is a low affinity site

A previous study (Kubo et al., 2010) showed that the upstream region of *Lhx3/4* binds Foxd in *Ciona*, using a chromatin immunoprecipitation assay in which Gfp-tagged Foxd protein was precipitated with an anti-Gfp antibody. To further confirm that Foxd binds to the site identified in our experiments, we performed an *in vitro* binding assay (electrophoresis mobility shift assay; EMSA). When the putative binding site around the −150 bp position was used as a probe, we observed a shifted band (Fig. 2A). This band was reduced after co-incubation of an unlabeled competitor with the same sequence as the probe, which suggests that the initial observed band was specific.

The shifted band observed here for the *Lhx3/4* binding site looked weak compared to those we had previously reported for a Foxd binding site in the upstream region of *Dmrt.a* (Tokuhiro et al., 2017). Therefore, we next examined whether there is a difference in the Foxd affinity of the repressive binding site in the *Dmrt.a* upstream region and the activating binding site in the *Lhx3/4* upstream region. To compare the affinity of these sites for Foxd, we used them as competitors in an EMSA assay in which the binding site from the *Dmrt.a* upstream region was used as a probe (Fig. 2B). We observed that the shifted band was weakened by incubation with a 50- or 100-fold molar excess of the *Dmrt.a* competitor, and disappeared with an 800-fold molar excess. In contrast, it was still visible with a 1600-fold molar excess of the *Lhx3/4* competitor. Notably, the *Lhx3/4* competitor competed more strongly than the same amount of a mutated version of the *Dmrt.a* competitor (μ*Dmrt.a*), indicating that the upstream region of *Lhx3/4* contains a weak Foxd binding site. By quantifying band strengths, we estimated that the

affinity of the repressive Foxd binding site of *Dmrt.a* is 8- to 16-fold stronger than that of the activating Foxd binding site of *Lhx3/4*, because incubation with a 50- or 100-fold molar excess of the *Dmrt.a* competitor and incubation with an 800-fold molar excess of the *Lhx3/4* competitor gave similar band strengths (Fig. 2B).

A region flanking the core binding site affects the strength of Foxd affinity

To identify the nucleotides which affect affinity to Foxd, we used various competitors in EMSA assays (Fig. 3A). There are five blocks of nucleotides that differ between the Foxd binding sites located upstream of *Lhx3/4* and *Dmrt.a*, which we here call blocks A to E (Fig. 3A). The competitor, LDDDL, in which blocks A and E are *Lhx3/4*-type and blocks B to D are *Dmrt.a*-type, effectively reduced the signal strength of the shifted band (lane 5 in Figure 3B, C). This suggests that blocks A and E are not critical for Foxd affinity. An additional block among blocks B to D was changed from the *Dmrt.a*- to the *Lhx3/4*-type in the next three competitors we tested—LDLDL, LLDDL, and LDDLL. The competitor LDDLL was found to be the most effective at reducing the signal strength of the shifted band. LLDDL was the least effective, and LDLDL was modestly effective. These observations indicate that block B is the most critical for Foxd affinity, followed by C, and then D. The results from three additional competitors—LDLLL, LLLDL, and LLDLL—in which one of the blocks B to D was *Dmrt.a*-type and the remaining blocks were *Lhx3/4*-type, further support this conclusion. That is, LDLLL, in which block B is *Dmrt.a*-type, was found to be most effective, and LLDLL, in which block C is *Dmrt.a*-type, was the second-most effective.

Differences in the nucleotide sequences of Foxd binding sites determine Foxd action

The above results demonstrate that the Foxd binding site of *Lhx3/4* is qualitatively

different to that of *Dmrt.a*. To test whether this qualitative difference causes Foxd to act as either an activator or a repressor, we first changed block B of the Foxd binding site in the *Lhx3/4* reporter construct into the *Dmrt.a*-type (i.e., the sequence of this site was changed into the sequence of the competitor LDLLL). As this mutated construct was not expressed at all (Fig. 4A, B), it is highly likely that this specific mutation changed the action of Foxd and caused it to act as a repressor—because a previous mutation introduced into the core binding sequence for Foxd at this site reduced, but did not abolish, reporter expression (see Figure 1A). For further confirmation, we inserted the sequence of the competitor LDLLL at nucleotide position −40, and left the original Foxd binding site intact. The expression of this reporter was significantly reduced (Fig. 4A, C). As a control, we inserted the sequence of an intact Foxd binding site in which all blocks were *Lhx3/4*-type (LLLLL). We observed that this construct was expressed in vegetal cells (Fig. 4A, D), and notably, ectopic expression was detected in marginal vegetal cells. Because the parents of these cells express *Foxd* (Imai et al., 2004; Imai et al., 2002), the insertion of an additional Foxd binding site might have made this region hyper-sensitive to Foxd, thereby enabling a response to a low level of Foxd even in the absence of nuclear β-catenin—which is required for *Lhx3/4* expression in normal embryos (Hudson et al., 2016; Satou et al., 2001).

The flanking regions of Foxd binding sites of known targets

As in the case of *Dmrt.a*, *Dlx.b* is expressed in the animal hemisphere and negatively regulated by Foxd in the vegetal hemisphere (Tokuhiro et al., 2017). Furthermore, a chromatin immunoprecipitation (ChIP) assay followed by deep-sequencing has shown that Gfp-tagged Foxd binds to the upstream region of *Dlx.b* (Tokuhiro et al., 2017). We identified a Foxd binding motif in this upstream region using the Patser program with the PWMs for human

FOXD2 and *Ciona* Foxd, and found that this region acted as a strong competitor in an EMSA assay using the Foxd binding site upstream of *Dmrt.a* as a probe (Fig. 5).

Conversely, *Zic-r.b* (previously called *ZicL*) is activated by Foxd and two putative Foxd binding sites have been identified in its upstream region using reporter assays (Anno et al., 2006). A weak, but statistically nonsignificant, peak was also detected in this region by ChIP assay (Tokuhiro et al., 2017). Of these sites, we used the one which gave a higher Patser score as a competitor and found that this region did not strongly compete with the *Dmrt.a* probe (Fig. 5)—as observed for the Foxd binding site of *Lhx3/4*. This observation supports the notion that, *in vitro*, activating Foxd sites bind Foxd weakly and repressive Foxd sites bind Foxd strongly.

To directly compare Foxd occupancy at these upstream regions *in vivo*, we performed quantitative PCR using ChIP samples from our previous study (Tokuhiro et al., 2017) and primers designed to amplify genomic regions that included the Foxd binding sites upstream of *Dmrt.a*, *Dlx.b*, *Lhx3/4*, and *Zic-r.b*. The upstream regions of *Dmrt.a*, *Dlx.b*, *Lhx3/4*, and *Zic-r.b* were enriched more than two-fold, while negative control regions within the *Pou2* and *Hey* loci (which are not expected to bind Foxd) were not enriched (Fig. 6). Enrichment of the upstream region of *Dmrt.a* was much greater than of the upstream regions of *Lhx3/4* and *Zic-r.b*, and the upstream region of *Dlx.b* was slightly more enriched than that of *Lhx3/4* or *Zic-r.b*. These observations suggest that the binding site affinities we observed *in vitro* are related to, but not determinative for, *in vivo* occupancy of Foxd.

Discussion

In ascidian embryogenesis *Foxd* plays a key role in stabilizing the animal-vegetal axis, which is first specified by maternal factors (Tokuhiro et al., 2017). Namely, *Foxd* is activated in the vegetal hemisphere by maternal factors, and then activates genes specific to the vegetal hemisphere while repressing genes specific to the animal hemisphere. Here, we have demonstrated that cis-regulatory elements determine the outcome of Foxd activity on its target genes. We discerned two types of Foxd binding elements *in vitro* by EMSA assays; target genes that have high affinity sites are repressed, and target genes that have low affinity sites are activated.

In ascidian embryos, *Foxd* is activated by nuclear β-catenin in cells which contributes to endodermal and mesodermal tissues (Imai et al., 2002). Many deuterostome animals similarly use nuclear β-catenin to specify endomesoderm (Funayama et al., 1995; Guger and Gumbiner, 1995; Heasman et al., 1994; Imai et al., 2000; Kelly et al., 1995; Logan et al., 1999; Schneider et al., 1996; Wikramanayake et al., 1998). In addition, downregulation of nuclear β-catenin results in expansion of the animal plate in sea urchin embryos (Yaguchi et al., 2008), and two β-catenin proteins redundantly repress expression of neural marker genes in zebrafish embryos (Bellipanni et al., 2006). These observations indicate that β-catenin-dependent mechanisms repress ectodermal fate in these animals (Range, 2014). It might be possible that Foxd acts similarly in these animals.

A previous study on Foxd in *Xenopus* embryos showed that the Engrailed-homology domain is necessary for its repressive function and that the acidic blob region is necessary for its activating function (Neilson et al., 2012). The Engrailed-homology domain is clearly conserved in ascidian Foxd (Tokuhiro et al., 2017). An additional domain, which is conserved among fish and amphibians, has also been reported to contribute to the repressive function of Foxd (Klein

et al., 2013). This domain is not conserved in *Ciona* Foxd, nor is the acidic blob domain. However, ascidian Foxd does contain an N-terminal region where acidic residues are enriched, and it is possible that this region may act similarly to the acidic blob domain to activate targets.

Although the Fox domain is the main DNA binding domain of Fox family transcription factors, additional domains may be required for binding to low- and high-affinity binding sites. Differences in Foxd-DNA conformation at low- and high-affinity sites may explain how Foxd can variously upregulate and downregulate its targets. A similar possibility has been suggested for the CTCF transcription factor by a study using ChIP assays; CTCF bound to low occupancy sites is likely to be involved in gene activation, while CTCF bound to high occupancy sites is likely to be involved in gene repression and to act as an insulator (Essien et al., 2009). It is thus possible that other multi-functional transcription factors may similarly bind to qualitatively different sites to fulfil different functions.

Meanwhile, as revealed in our ChIP assay, Foxd occupancy *in vivo* may not directly relate to the mode of Foxd function. For example, multiple low-affinity sites may collectively recruit Foxd at a high frequency. Indeed, our reporter assay (Figure 1) indicates multiple Foxd binding sites in the upstream region of *Lhx3/4*.

In vitro binding assays have suggested that some transcription factors can recognize two or more distinct motifs (Badis et al., 2009; Franco-Zorrilla et al., 2014), although some of these observations may be explained by monomeric and dimeric binding (Jolma et al., 2013). Here, we identified that the core sequences of two qualitatively different Foxd binding sites were similar to each other, while their flanking sequences were different. The flanking sequence of the Foxd binding site in the *Lhx3/4* upstream region is similar to the core Foxd binding motif and is recognized as a binding site with the *Ciona* PWM. Therefore, it is possible that this site binds two Foxd molecules,

which might form a dimer, although the flanking region of the Foxd binding site in the *Zic-r.b* upstream region is not similar to the core Foxd binding motif. Our data show that these two qualitatively different Foxd binding motifs evoke different Foxd functions, and thus, that cis-regulatory sequences regulate the mode of Foxd activity.

Materials and Methods

Animals, whole-mount *in situ* hybridization, and gene identifiers

Ciona intestinalis (type A; also called *Ciona robusta*) adults were obtained from the National Bio-Resource Project for *Ciona*. cDNA clones were obtained from our EST clone collection (Satou et al., 2005). Whole-mount *in situ* hybridization was performed as described previously (Imai et al., 2004). Identifiers of genes examined in the present study are CG.KY.Chr13.449 for *Lhx3/4*, CG.KY.Chr5.698 for *Dmrt.a*, CG.KY.Chr7.359 for *Dlx.b*, CG.KY.Chr6.26/27/28/29/30/31 for *Zic-r.b*, CG.KY.Chr1.1698 for *Macho-1*, CG.KY.Chr4.359 for *Pou2f*, and CG.KY.Chr10.1431 for *Hey*.

Reporter assays

Reporter constructs were introduced into fertilized eggs by electroporation. Chromosomal positions of the upstream sequences for reporter constructs and the mutated sequence are indicated in Figure 1. We randomly chose embryos electroporated with reporter constructs to examine reporter construct expression by *in situ* hybridization. All reporter assays were performed at least twice with different batches of embryos.

Electrophoresis mobility shift assay (EMSA)

Recombinant Foxd.b protein was produced as a fusion of the Foxd DNA-binding domain and glutathione S-transferase in *Escherichia coli* BL21 star DE3 (Thermo Fisher Scientific), and purified under native conditions using glutathione Sepharose 4B (GE Healthcare) (Tokuhiro et al., 2017). After annealing two complementary oligonucleotides, the protruding ends were filled with biotin-11-dUTP, and this biotin-labelled double-stranded oligonucleotide was used as a probe. Proteins and the biotin-labeled probe were mixed in 10 mM Tris (pH 7.5), 50 mM KCl, 1 mM DTT, 1 mM EDTA, 50 ng/μL poly (dIdC), 2.5% glycerol, and 0.05% NP40, with or without competitor double-stranded DNAs. Proteins amounts were empirically determined. Protein-DNA complexes were detected using an AP-conjugated anti-biotin antibody (Roche) and CDP-star substrate (Roche). Oligonucleotides used for the intact Foxd binding sites in the upstream regions of *Lhx3/4* and *Dmrt.a* were as follows: *Lhx3/4*, 5′-aaaAAACACCGCTGTTTGCATTGTG-3′ and 5′-aaaCACAATGCAAACAGCGGTGTTT-3′; *Dmrt.a*, 5′-aaaTAACAATAATGTTTACGTTGGT-3′ and 5′-aaaACCAACGTAAACATTATTGTTA-3′. Nucleotide sequences of other competitors are shown in Figures 2, 3, and 5. Bands were quantified as arbitrary units using an imager (ChemiDoc XRS, Bio-Rad) and Quantity-One software (Bio-Rad).

Chromatin immunoprecipitation

Embryos electroporated with a DNA construct encoding GFP-tagged Foxd under the control of the *Foxd* promoter were fixed at the 32-cell stage. Chromatin-immunoprecipitation was performed using an anti-Gfp antibody and precipitated DNA was amplified by ligation-mediated PCR (Kubo et al., 2010). Whole-cell extract DNA was used as a control. Quantitative PCR was used to measure the enrichment of five regions using the following primers: the Foxd binding site in the upstream region of *Dmrt.a*, 5′-TCAATTTAAAACCCGTCGACAA-3′ and 5′-

ATGTACATTGCCACAACAACCAA-3′; the Foxd binding site in the upstream region of *Lhx3/4*, 5′-CGTCGTCTGTACCGCATTATGA-3′ and 5′-ACAATTAACGCCTCGCTTTGA-3′; the Foxd binding site in the upstream region of *Dlx.b*, 5′-ACTCACTTGAATAAAGCCGAAGAGA-3′ and 5′- GCTCGAGCACGTGCATTGT-3′; the Foxd binding site in the upstream region of *Zic-r.b*, 5′-GCGAAAGCGTGCCAAAAGTA-3′ and 5′-CCCCACCTCCGATATTTGC -3′; a control region within the *Macho-1* (*Zic-r.a*) locus, 5′-GTACTCTCCAATGCGTCAATCCA-3′ and 5′-TCGCACGCCAATTAAATGC-3′; a control region within the *Hey* locus, 5′-TGTTACGCGGAAGTGTTTCATT-3′ and 5′-CCTTGGTGCCGGAAATTAAAA-3′; a control region within the *Pou2* locus, 5′-ATGTGCAGAAGGAGCAATCAA-3′ and 5′-CCCACCAAGTCCTCAGGTACAT-3′. Enrichment was calculated using the control region within the *Macho-1* locus as an internal reference.

Acknowledgment

A draft of this manuscript was edited by Edanz Group. This research was supported by the Japan Society for the Promotion of Science [grant numbers 17KT0020 and 18J14588].

References

Anno, C., Satou, A., Fujiwara, S., 2006. Transcriptional regulation of ZicL in the Ciona intestinalis embryo. Dev Genes Evol 216, 597-605.

Badis, G., Berger, M.F., Philippakis, A.A., Talukder, S., Gehrke, A.R., Jaeger, S.A., Chan, E.T., Metzler, G., Vedenko, A., Chen, X.Y., Kuznetsov, H., Wang, C.F., Coburn, D., Newburger, D.E., Morris, Q., Hughes, T.R., Bulyk, M.L., 2009. Diversity and Complexity in DNA Recognition by Transcription Factors. Science 324, 1720-1723.

Behrens, J., vonKries, J.P., Kuhl, M., Bruhn, L., Wedlich, D., Grosschedl, R., Birchmeier, W., 1996. Functional interaction of beta-catenin with the transcription factor LEF-1. Nature 382, 638-642.

Bellipanni, G., Varga, M.T., Maegawa, S., Imai, Y., Kelly, C., Myers, A.P., Chu, F., Talbot, W.S., Weinberg, E.S., 2006. Essential and opposing roles of zebrafish beta-catenins in the formation of dorsal axial structures and neurectoderm. Development 133, 1299-1309.

Cavallo, R.A., Cox, R.T., Moline, M.M., Roose, J., Polevoy, G.A., Clevers, H., Peifer, M., Bejsovec, A., 1998. Drosophila Tcf and Groucho interact to repress Wingless signalling activity. Nature 395, 604-608.

Essien, K., Vigneau, S., Apreleva, S., Singh, L.N., Bartolomei, M.S., Hannenhalli, S., 2009. CTCF binding site classes exhibit distinct evolutionary, genomic, epigenomic and transcriptomic features. Genome Biol 10, R131.

Franco-Zorrilla, J.M., Lopez-Vidriero, I., Carrasco, J.L., Godoy, M., Vera, P., Solano, R., 2014. DNA-binding specificities of plant transcription factors and their potential to define target genes. Proceedings of the National Academy of Sciences of the United States of America 111, 2367-2372.

Funayama, N., Fagotto, F., Mccrea, P., Gumbiner, B.M., 1995. Embryonic Axis Induction by the Armadillo Repeat Domain of β-Catenin - Evidence for Intracellular Signaling. The Journal of cell biology 128, 959-968.

Guger, K.A., Gumbiner, B.M., 1995. Beta-Catenin Has Wnt-Like Activity and Mimics the Nieuwkoop Signaling Center in Xenopus Dorsal-Ventral Patterning. Developmental Biology 172, 115-125.

Heasman, J., Crawford, A., Goldstone, K., Garnerhamrick, P., Gumbiner, B., Mccrea, P., Kintner, C., Noro, C.Y., Wylie, C., 1994. Overexpression of Cadherins and Underexpression of Beta-Catenin Inhibit Dorsal Mesoderm Induction in Early Xenopus Embryos. Cell 79, 791-803.

Hudson, C., Sirour, C., Yasuo, H., 2016. Co-expression of Foxa.a, Foxd and Fgf9/16/20 defines a transient mesendoderm regulatory state in ascidian embryos. Elife 5, e14692.

Imai, K., Takada, N., Satoh, N., Satou, Y., 2000. β-catenin mediates the specification of endoderm cells in ascidian embryos. Development 127, 3009-3020.

Imai, K.S., Hino, K., Yagi, K., Satoh, N., Satou, Y., 2004. Gene expression profiles of transcription factors and signaling molecules in the ascidian embryo: towards a comprehensive understanding of gene

networks. Development 131, 4047-4058.

Imai, K.S., Satoh, N., Satou, Y., 2002. An essential role of a FoxD gene in notochord induction in Ciona embryos. Development 129, 3441-3453.

Jolma, A., Yan, J., Whitington, T., Toivonen, J., Nitta, K.R., Rastas, P., Morgunova, E., Enge, M., Taipale, M., Wei, G.H., Palin, K., Vaquerizas, J.M., Vincentelli, R., Luscombe, N.M., Hughes, T.R., Lemaire, P., Ukkonen, E., Kivioja, T., Taipale, J., 2013. DNA-Binding Specificities of Human Transcription Factors. Cell 152, 327-339.

Kelly, G.M., Erezyilmaz, D.F., Moon, R.T., 1995. Induction of a Secondary Embryonic Axis in Zebrafish Occurs Following the Overexpression of Beta-Catenin. Mechanisms of Development 53, 261-273.

Klein, S.L., Neilson, K.M., Orban, J., Yaklichkin, S., Hoffbauer, J., Mood, K., Daar, I.O., Moody, S.A., 2013. Conserved structural domains in FoxD4L1, a neural forkhead box transcription factor, are required to repress or activate target genes. PLoS One 8, e61845.

Kubo, A., Suzuki, N., Yuan, X., Nakai, K., Satoh, N., Imai, K.S., Satou, Y., 2010. Genomic cis-regulatory networks in the early Ciona intestinalis embryo. Development 137, 1613-1623.

Logan, C.Y., Miller, J.R., Ferkowicz, M.J., McClay, D.R., 1999. Nuclear β-catenin is required to specify vegetal cell fates in the sea urchin embryo. Development 126, 345-357.

Meijsing, S.H., Pufall, M.A., So, A.Y., Bates, D.L., Chen, L., Yamamoto, K.R., 2009. DNA Binding Site Sequence Directs Glucocorticoid Receptor Structure and Activity. Science 324, 407-410.

Molenaar, M., vandeWetering, M., Oosterwegel, M., PetersonMaduro, J., Godsave, S., Korinek, V., Roose, J., Destree, O., Clevers, H., 1996. XTcf-3 transcription factor mediates beta-catenin-induced axis formation in Xenopus embryos. Cell 86, 391-399.

Neilson, K.M., Klein, S.L., Mhaske, P., Mood, K., Daar, I.O., Moody, S.A., 2012. Specific domains of FoxD4/5 activate and repress neural transcription factor genes to control the progression of immature neural ectoderm to differentiating neural plate. Dev Biol 365, 363-375.

Oda-Ishii, I., Abe, T., Satou, Y., 2018. Dynamics of two key maternal factors that initiate zygotic regulatory programs in ascidian embryos. Dev Biol 437, 50-59.

Oda-Ishii, I., Kubo, A., Kari, W., Suzuki, N., Rothbacher, U., Satou, Y., 2016. A maternal system initiating the zygotic developmental program through combinatorial repression in the ascidian embryo. PLoS genetics 12, e1006045.

Range, R., 2014. Specification and positioning of the anterior neuroectoderm in deuterostome embryos. Genesis 52, 222-234.

Roose, J., Molenaar, M., Peterson, J., Hurenkamp, J., Brantjes, H., Moerer, P., van de Wetering, M., Destree, O., Clevers, H., 1998. The Xenopus Wnt effector XTcf-3 interacts with Groucho-related transcriptional repressors. Nature 395, 608-612.

Rothbächer, U., Bertrand, V., Lamy, C., Lemaire, P., 2007. A combinatorial code of maternal GATA, Ets and β-catenin-TCF transcription factors specifies and patterns the early ascidian ectoderm.

Development 134, 4023-4032.

Sandelin, A., Alkema, W., Engstrom, P., Wasserman, W.W., Lenhard, B., 2004. JASPAR: an open-access database for eukaryotic transcription factor binding profiles. Nucleic Acids Res 32, D91-94.

Satou, Y., Imai, K.S., Satoh, N., 2001. Early embryonic expression of a LIM-homeobox gene Cs-lhx3 is downstream of beta-catenin and responsible for the endoderm differentiation in Ciona savignyi embryos. Development 128, 3559-3570.

Satou, Y., Kawashima, T., Shoguchi, E., Nakayama, A., Satoh, N., 2005. An integrated database of the ascidian, Ciona intestinalis: Towards functional genomics. Zool Sci 22, 837-843.

Schneider, S., Steinbeisser, H., Warga, R.M., Hausen, P., 1996. beta-Catenin translocation into nuclei demarcates the dorsalizing centers in frog and fish embryos. Mechanisms of Development 57, 191-198.

Surjit, M., Ganti, K.P., Mukherji, A., Ye, T., Hua, G., Metzger, D., Li, M., Chambon, P., 2011. Widespread Negative Response Elements Mediate Direct Repression by Agonist-Liganded Glucocorticoid Receptor. Cell 145, 224-241.

Tokuhiro, S., Tokuoka, M., Kobayashi, K., Kubo, A., Oda-Ishii, I., Satou, Y., 2017. Differential gene expression along the animal-vegetal axis in the ascidian embryo is maintained by a dual functional protein Foxd. PLoS genetics 13, e1006741.

Vincentelli, R., Cimino, A., Geerlof, A., Kubo, A., Satou, Y., Cambillau, C., 2011. High-throughput protein expression screening and purification in Escherichia coli. Methods 55, 65-72.

Wikramanayake, A.H., Huang, L., Klein, W.H., 1998. beta-Catenin is essential for patterning the maternally specified animal-vegetal axis in the sea urchin embryo. Proc Natl Acad Sci U S A 95, 9343-9348.

Yaguchi, S., Yaguchi, J., Angerer, R.C., Angerer, L.M., 2008. A Wnt-FoxQ2-nodal pathway links primary and secondary axis specification in sea urchin embryos. Developmental Cell 14, 97-107.

Figure legends

Figure 1. Identification of Foxd binding sites in the upstream region of *Lhx3/4*. (A) A series of deletion reporter constructs and two mutation reporter constructs containing the upstream region of *Lhx3/4* were examined. Numbers of cells with reporter expression in individual embryos are shown by dots (results from different experiments are shown by different colors for each construct), and mean values are shown by thick black lines. Wilcoxon rank sum tests were performed using numbers of cells with reporter expression in individual embryos, and p-values less than 0.01 are shown on the right by two asterisks; ns, no significant change. (B) The nucleotide sequence of the upstream region and the region around the transcription start site of *Lhx3/4*. Putative Foxd binding sites identified using the Patser program and position weight matrices for human FOXD2 (JASPAR database, MA0847.1) (Jolma et al., 2013; Sandelin et al., 2004), and *Ciona* Foxd (Vincentelli et al., 2011), are underlined and enclosed by cyan boxes, respectively. Sequence logos are presented below. Mutated nucleotide sequences in the mutant constructs are shown in magenta. (C, D) *In situ* hybridization to detect reporter expression in embryos electroporated with (C) a construct containing a mutation in the Foxd site around nucleotide position −150 and (D) a construct containing mutations in all putative Foxd binding sites. μFoxd sites, mutated Fox sites**.**

Figure 2. The affinity of the Foxd binding site upstream of *Lhx3/4* is weak. (A) An EMSA analysis confirming that the identified Foxd binding site binds Foxd *in vitro*. Quantification of the shifted bands is shown below. (B) An EMSA assay showing that the Foxd binding site upstream of *Dmrt.a* has a higher affinity for Foxd than that upstream of *Lhx3/4*. Various amounts of three competitors (shown at the top) were added to the reaction. Quantification of the shifted bands is shown below.

Figure 3. Identification of nucleotides that affect Foxd affinity by an EMSA assay. (A) Competitors used in the assay. On the basis of the differences in binding sites and flanking regions, five blocks were defined. (B) The competitors shown in (A) were added to the reactions of an EMSA assay. (C) Quantification of the shifted bands shown in (B).

Figure 4. A high affinity site and a low affinity site act as repressing and activating sites, respectively. (A) Numbers of cells with reporter expression per embryo are shown by dots (results from different experiments are shown by cyan and magenta), and mean values are shown by thick black lines. Wilcoxon rank sum tests were performed using numbers of cells with reporter expression in individual embryos, and p-values were less than 0.01, and are shown on the right by two black asterisks. Embryos electroporated with the fourth construct showed ectopic reporter expression in A6.2 cells (shown by arrows). (B–D) *In situ* hybridization to detect reporter expression in embryos electroporated with (B) the second construct containing a LDLLL site, (C) the third construct containing LLLLL and LDLLL sites, and (D) the fourth construct containing two LLLLL sites. In (D), ectopic expression is shown by an arrowhead.

Figure 5. Foxd binding sites in the upstream sequences of *Dlx.b* and *Zic-r.b*, which are negatively and positively regulated by Foxd, respectively. (A) Comparison of Foxd binding sites in the upstream sequences of *Dmrt.a, Dlx.b, Zic-r.b*, and *Lhx3/4*. (B) An EMSA assay to examine the Foxd affinity of binding sites in the upstream sequences of *Dlx.b* and *Zic-r.b*. (C) Quantification of the shifted bands shown in (B).

Figure 6. *In vivo* occupancy of Foxd in the upstream regions of *Dmrt.a*, *Dlx.b*, *Lhx3/4*, and *Zic-r.b*. The enrichment of genomic regions containing Foxd binding sites was measured by chromatin immunoprecipitation (ChIP) assays followed by quantitative PCR. The ChIP assay was performed

using an anti-Gfp antibody and 32-cell embryos electroporated with a construct designed to express mRNA encoding Gfp-tagged Foxd under the control of the *Foxd* upstream regulatory region (Kubo et al., 2010). A genomic region within the *Macho-1* locus was used as an internal reference. *Pou2* and *Hey* were used as negative controls. Two biological replicates were performed and are represented by different colors.

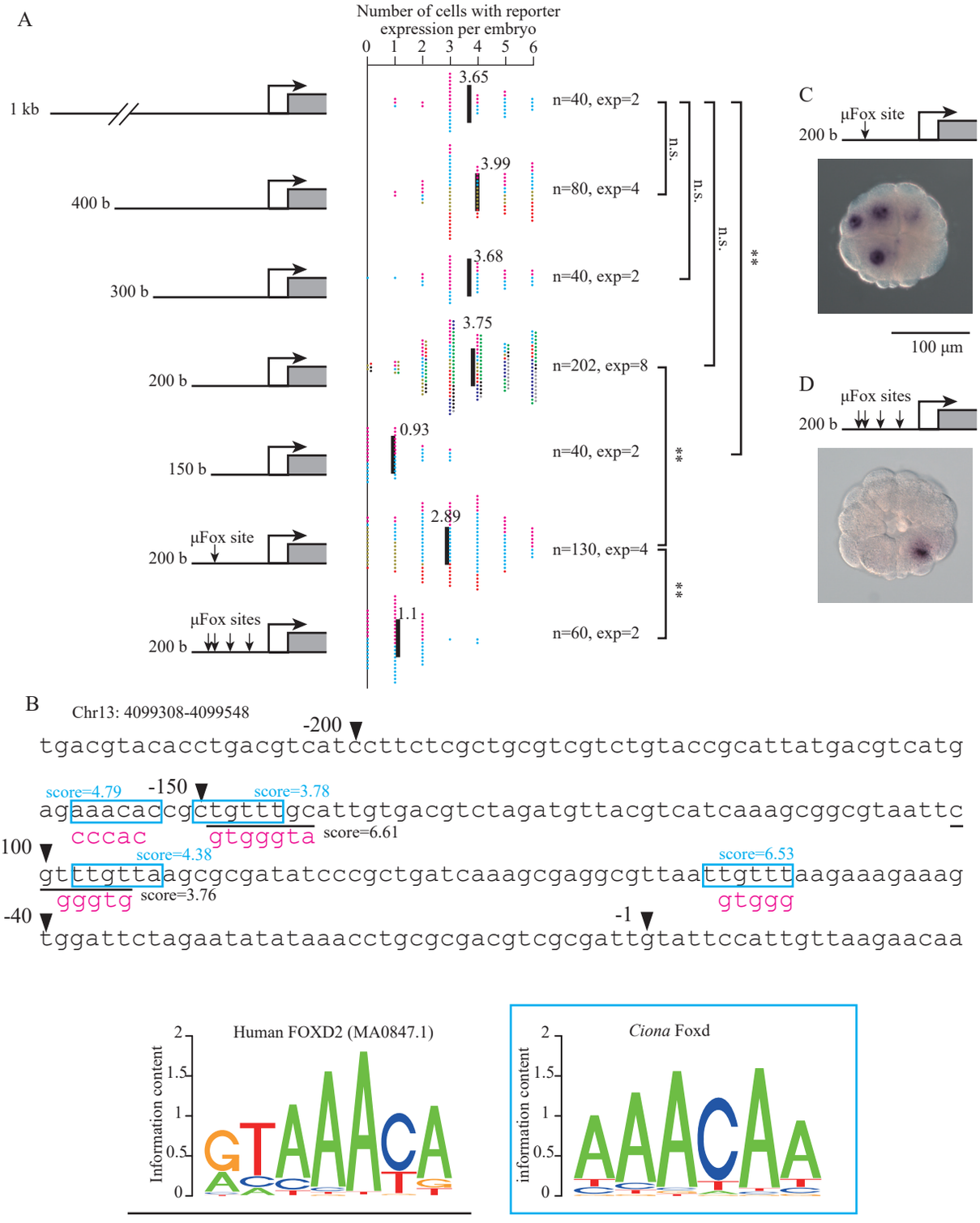
A
Number of cells with reporter expression per embryo
0 1 2 3 4 5 6
1 kb
400 b
300 b
200 b
150 b
µFox site
200 b
µFox sites
200 b
3.65
3.99
3.68
3.75
0.93
2.89
1.1
n=40, exp=2
n=80, exp=4
n=40, exp=2
n=202, exp=8
n=40, exp=2
n=130, exp=4
n=60, exp=2
n.s.
n.s.
n.s.
**
**
**
C
µFox site
200 b
100 µm
D
µFox sites
200 b
B
Chr13: 4099308-4099548
-200
tgacgtacacctgacgtcatccttctcgctgcgtcgtctgtaccgcattatgacgtcatg
score=4.79
-150
score=3.78
agaaacaccgctgtttgcattgtgacgtctagatgttacgtcatcaaagcggcgtaattc
cccac
gtgggta
score=6.61
-100
score=4.38
score=6.53
gttttgttaagcgcgatatcccgctgatcaaagcgaggcgttaattgtttaagaaagaaag
gggtg
score=3.76
gtggg
-40
-1
tggattctagaatatataaacctgcgcgacgtcgcgattgtattccattgttaagaacaa
Human FOXD2 (MA0847.1)
Information content
2
1.5
1
0.5
0
Ciona Foxd
information content
2
1.5
1
0.5
0

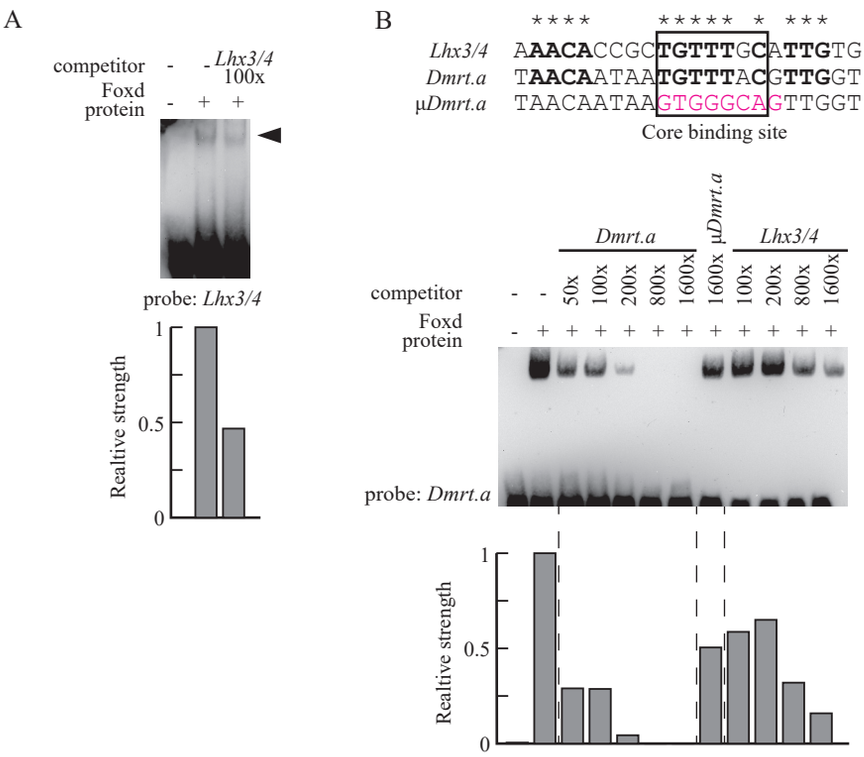
A
competitor - - Lhx3/4
100x
Foxd
protein - + +
probe: Lhx3/4
Realtive strength
1
0.5
0
B
* * * * * * * * * * * * *
Lhx3/4 AAACACCGCTGTTTGCATTGTG
Dmrt.a TAACAATAATGTTTACGTTGGT
μDmrt.a TAACAATAAGTGGGCAGTTGGT
Core binding site
Dmrt.a
μDmrt.a
Lhx3/4
competitor - - 50x 100x 200x 800x 1600x 1600x 100x 200x 800x 1600x
Foxd
protein - + + + + + + + + + + +
probe: Dmrt.a
Realtive strength
1
0.5
0

A

lane	competitor	sequence (magenta, Dmrt.a specific nucleotides; cyan, Lhx3/4 specific nucleotides)
3	*Dmrt.a*	TAACAATAATGTTTACGTTGGT
4	μ*Dmrt.a*	TAACAATAAGTGGGCAGTTGGT
5	LDDDL	AAACAATAATGTTTACGTTGTG
6	LDLDL	AAACAATAATGTTTGCGTTGTG
7	LLDDL	AAACACCGCTGTTTACGTTGTG
8	LDDLL	AAACAATAATGTTTACATTGTG
9	LDLLL	AAACAATAATGTTTGCATTGTG
10	LLLDL	AAACACCGCTGTTTGCGTTGTG
11	LLDLL	AAACACCGCTGTTTACATTGTG
12	*Lhx3/4*	AAACACCGCTGTTTGCATTGTG
	block	A B C D E

Core binding site

B

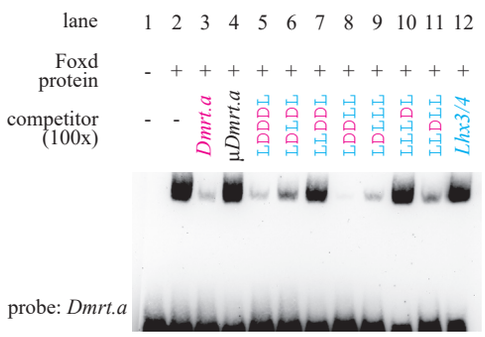

C

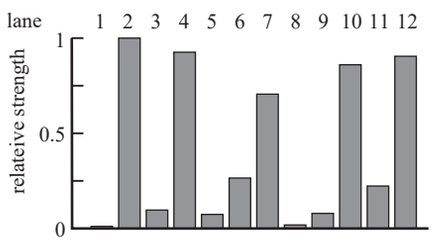

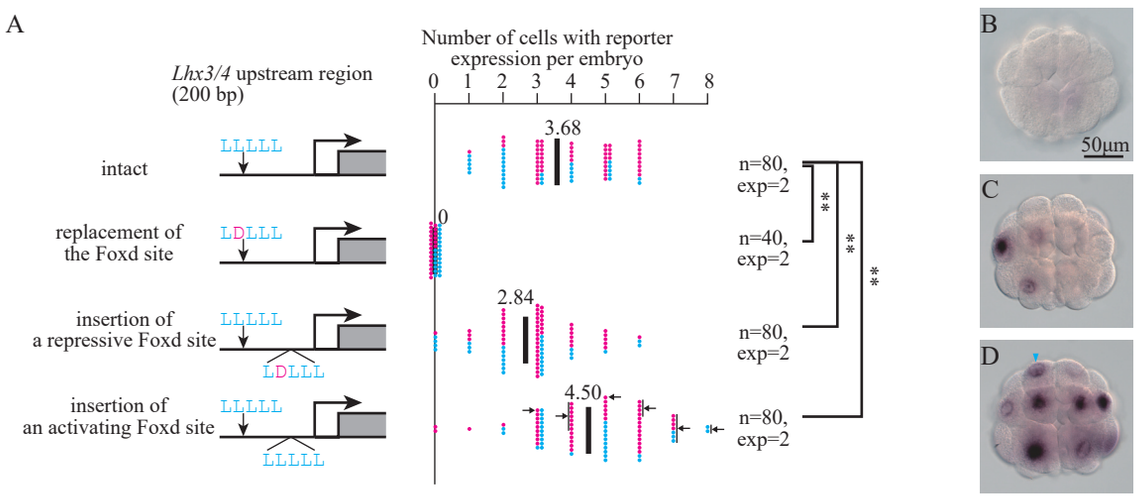
A
Lhx3/4 upstream region
(200 bp)
intact
LLLLL
replacement of
the Foxd site
LDLLL
insertion of
a repressive Foxd site
LLLLL
LDLLL
insertion of
an activating Foxd site
LLLLL
LLLLL
Number of cells with reporter
expression per embryo
0 1 2 3 4 5 6 7 8
3.68
0
2.84
4.50
n=80,
exp=2
n=40,
exp=2
n=80,
exp=2
n=80,
exp=2
**
**
**
B
50µm
C
D

A

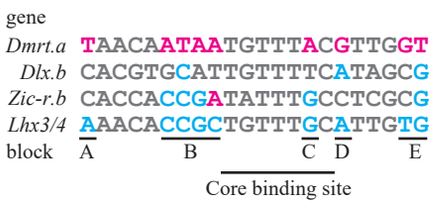
gene
Dmrt.a TAACAATAATGTTTACGTTGGT
Dlx.b CACGTGCATTGTTTTTCATAGCG
Zic-r.b CACCACCGATATTTGCCTCGCG
Lhx3/4 AAACACCGCTGTTTTGCATTGTG
block A B C D E
Core binding site

B

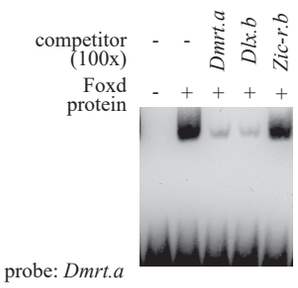
competitor (100x) - - Dmrt.a Dlx.b Zic-r.b
Foxd protein - + + + +
probe: Dmrt.a

C

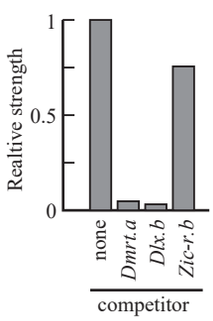
Realtive strength
1
0.5
0
none
Dmrt.a
Dlx.b
Zic-r.b
competitor

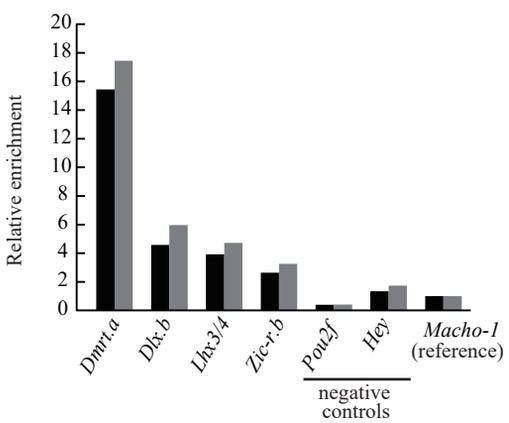
Relative enrichment
20
18
16
14
12
10
8
6
4
2
0
Dmrt.a
Dlx.b
Lhx3/4
Zic-r.b
Pou2f
Hey
Macho-1
(reference)
negative
controls